Experimental investigation and numerical simulation on the effect of fissure water pressure in vertical sliding surface

ZHANG Lei[1,2], LI Shihai[1], LIAN Zhenzhong[1,2] & WANG Yuannian[1]

1. Institute of Mechanics, Chinese Academy of Sciences, Beijing 100080, China;
2. Graduate School, Chinese Academy of Sciences, Beijing 100060, China
Correspondence should be addressed to Li Shihai (email: shli@imech.ac.cn)
Received April 25, 2005

Abstract This paper studies the effect of fissure water pressure in different fractures on the critical angle of landslide by laboratory investigation and numerical simulation in order to understand the mechanisms of fissure water pressure on landslide stability. Laboratory observations show that the effect of fissure water pressure on the critical angle of landslide is little when the distance between water-holding fracture and slope toe is three times greater than the depth of fissure water. These experimental results are also simulated by a three-dimensional face-to-face contact discrete element method. This method has included the fissure water pressure and can accurately calculate the critical angle of jointed slope when fissure water pressure in vertical sliding surface exists. Numerical results are in good agreement with experimental observations. It is revealed that the location of water-holding structural surface is important to landslide stability. The ratio of the distance between water-holding fissure and slope toe to the depth of fissure water is a key parameter to justify the effect of fissure water pressure on the critical angle of landslide.

Keywords: jointed rock slope, discrete element method, fracture in vertical sliding surface, model experiment, fissure water pressure.

DOI: 10.1360//04zze9

1 Introduction

Rock slopes usually contain many structural surfaces in geological engineering. However, the mechanism of rock slope failure has not been profoundly understood. Therefore, it is important to deeply analyze the failure mechanism and stability of such rock slopes through experimental investigation and numerical simulation. Previous site investigations show that water is one of the key factors to induce landslide[1−5]. "No landslide without water" vividly points out the importance of water in the sliding mechanisms of rock slopes. What is the primary mechanism of water-induced landslide

has been a hot topic in engineering geology and rock engineering. Ref. [1] pointed out that water has two functions in the mechanisms of landslides: First, water can reduce the shear strength of materials[6] on the slide surface; second, water will produce additional pushing force in the sliding force and reduce the effective stress on the slide surface.

Rock mass is different from other engineering materials[7]. As geologic material, rock mass is formed through lengthy geologic years, enduring different geologic effects and tectonic forces. Rock mass contains many joints, faults and fissures. These joints control rock structures, thus being the major failure mechanism of rock mass. Cracking structural surfaces induce distinct reduction of the mechanical characteristics and strong anisotropy. The permeability of rock mass mainly depends on the network development of joints and intersection characteristics and directivity of cracking structural surfaces. Hence fracture network model is more practical than homogeneous seepage model[8−10]. Flow through fractures simultaneously applies normal hydrostatic pressure (or fissure water pressure) and tangential pressure on fracture walls. Tangential pressure is usually small and ignorable. Zhang[11] discussed the effect of seepage pressure in jointed rock slope by means of fracture network model. He found that the shear strength of jointed rock mass was reduced by water and the sliding force was increased. If a jointed rock mass is almost in limiting equilibrium, seepage water (such as rain) will induce the sliding of rock mass. Shen[12] discussed some conceptual confusions on the usage of seepage pressure in engineering. Therefore, the effect of fissure water pressure on slope stability is not well understood.

The effect of fissure water on landslide stability mainly has two aspects[13]. First, fissure water softens interface or rock mass, that is, the water reduces the shear strength of soft interlayer in joints. Water softening may be reinforced due to high permeability of soft interlayer and tectonic movement. Second, fissure water may produce a pushing force along sliding direction and generate fissure water pressure in sliding surface. The pushing force adds to the sliding force, and the fissure water pressure reduces the effective stress in sliding surface, reducing frictional force to resist sliding. Therefore, fissure water is disadvantageous to landslide stability. The above-mentioned three effects are not easily distinguished in engineering, and an integrated effect is also difficultly obtained. One method is to individually analyze the effect of each factor on landslide stability.

This paper explores the effect of fissure water on the stability of jointed rock slope from both laboratory investigation and numerical simulations. The effect of fissure water in different positions is studied. Results show that the ratio of the distance between water-holding fracture and slope toe to the depth of fissure water is the major factor to the critical angle of landslide. When the ratio is larger than three, the pushing force from the fissure water is ignorable. A theoretical formula is also developed to express the relationship of spatial distribution of fissure water and the critical angle of landslide. A three-dimensional discrete element face-to-face contact model is incorporated with fissure water pressure and employed to simulate the experiment results.

2 Laboratory experiment

2.1 Experiment setup and procedure

An experiment is setup to investigate the effect of fissure water pressure on the landslide stability (see Fig. 1). This is a glass box whose walls are transparent. This box has the internal dimensions of 2000 mm×800 mm×1100 mm in length, width and height. The wall thickness is 20 mm. A rock slope is stacked with granite blocks that have the same dimensions of 200 mm×100 mm×100 mm and smooth surface. The slope has straight joint configuration stacked as follows: three blocks in width direction, seven blocks in length direction and five blocks in height direction. Total length is L=1.4 m and total height is H=0.5 m. Further, a layer of big blocks are laid and fixed to the bottom and sidewalls of this box. Then the above layers are laid according to the pre-designated joint configuration. Such a layout does not touch the box sidewall. A thin layer of sand is laid on the interface of blocks. The density of granite is ρ=2.7 kg/m^3, and the friction angle (ϕ) for interface varies from 18° to 21° due to variable sand sizes. The cohesion is C = 0. A pulley is fixed on the upper front wall to level this glass box. When a rock slope is ready, slowly incline the box through the pulley until slope slides or fails. A flexible water bag is pre-inserted into one of the vertical joints or sliding surfaces. This water bag is connected with water box through a pipe for water filling. The top of water bag is open and is fixed at a little higher position than the top surface of slope. Another water pipe is buried at the same height as the top surface of slope. When the water level in water bag is higher than the top surface of slope, water will automatically overflow. This can ensure that fissure water is in the same height as the top surface of slope before the slope strongly slides. A high-speed camera is used to capture the failure process. These photos are used for further numerical simulation and theoretical analysis.

Fig. 1. Experiment setup.

2.2 Experimental results and analysis

Seven types of experimental tests are carried out, each repeated three times. In the

first type of experiment, water is not added to the water bag, while in the other six tests, water is added to the water bag at different fractures from left to right in Fig. 1. The effect of fissure water pressure can be observed at different locations on the critical angle of landslide. Although water supply guarantees the water level before slope sliding, lowering down of water level can still be observed when the slope slides. Table 1 shows the experimental results where H_{water} is the depth of fissure water at limit equilibrium.

Table1 Experiment results

Watering fracture	First	Second	Third	Fourth	Fifth	Sixth	No watering
Critical angle (deg)	4.5	13.5	15.3	16.1	16.6	17.5	18.9
Critical angle (deg)	4.6	13.4	15.6	16.4	16.6	17.5	18.3
Critical angle (deg)	4.3	13.0	15.3	16.4	16.9	17.2	18.1
Average (deg)	4.5	13.3	15.4	16.3	16.7	17.4	18.4
H_{water}(m)	0.35	0.35	0.35	0.35	0.35	0.35	0

Experimental observations show that slope failure always begins from block sliding. Because the friction angle of each block is a little different, which block slides first is random. However, sliding of one block will cause the sliding of other blocks, making one column of blocks offset and finally toppling. The failure mode varies a little with different locations of water bag. The observed failure modes include sliding, toppling, and their combination. When a fracture is watered, the slope in the front is destroyed and the columns at the back are not affected. This is because the fissure water pressure pushes the front slope along sliding surface. When the whole slope is dry, the critical angle is 18.4 degree, which is close to the lower limit of friction angle of interface. When some block with smallest friction slides, all other blocks follow, producing global failure of slope. Therefore, we cannot simply use one criterion of sliding or toppling to judge the limiting equilibrium of a rock slope.

3 Numerical model and fundamental equations

3.1 Discrete element face-to-face contact model with fissure water pressure

In this discrete element method (DEM), a rock slope is assumed to be stacked by rock blocks which are intersected by discontinuity surfaces such as joints. Blocks contact each other with face-to-face modes[14,15]. This DEM observes the following hypotheses:

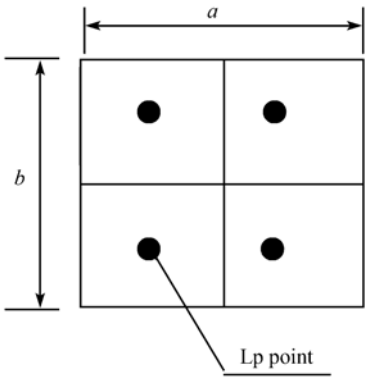

Fig. 2. Lp points for block.

(1) Each block is rigid. Its motion follows Newton's second law.

(2) Each interface is divided into four equal areas to describe the non-uniform force on the interface and calculate the torque of element. The force in each area is homogeneous and acts at its center denoted as Lp (see Fig. 2).

(3) Interaction of two neighboring blocks is described by normal and tangential stiffness. That is, normal and shear springs are assigned to each contact point. These springs prevent one block from penetrating into the other. Interface is frictional and follows Mohr-Coulomb's law. No tension is allowed.

(4) Fissure water pressure is expressed by a normal force P at the Lp point.

$$P = \iint_s p_s ds, \tag{1}$$

$$P_s = \gamma H, \tag{2}$$

where H is the height of the fissure water, s is the area of the Lp zone.

3.2 Fundamental equations of block motions

The DEM is based on discontinuity analysis, thus no compatibility of deformation is required along the interface of block assembly. The fundamental equations of block motions are as follows.

(1) Equation of motion. The forces on each block have external force, contacting forces from neighboring blocks, and fissure water pressure. The equations of motion for the ith block are as follows:

$$m^i \ddot{\vec{u}}^i + c_m \dot{\vec{u}}^i + c_k \sum_{j=1}^{n} (\dot{\vec{u}}^i - \dot{\vec{u}}^j) + k \sum_{j=1}^{n} (\vec{u}^i - \vec{u}^j) + \sum_{l=1}^{n_1} p^{i,l} = \vec{F}, \tag{3}$$

$$I^i \ddot{\vec{\theta}}^i + c_I r_0^2 \dot{\vec{\theta}}^i + c_k \sum_{l=1}^{n_1} \{\vec{r}_l \times [(\dot{\vec{\theta}}^i - \dot{\vec{\theta}}^j) \times \vec{r}_l]\} + k \sum_{l=1}^{n_1} \{\vec{r}_l \times [(\vec{\theta}^i - \vec{\theta}^j) \times \vec{r}_l]\} + \sum_{l=1}^{n_1} (\vec{r}_l \times p^{i,l}) = \vec{M}, \tag{4}$$

where m^i, I^i are the mass and inertia of ith block, $\vec{u}^i$, $\dot{\vec{u}}^i$, $\vec{\theta}^i$, $\dot{\vec{\theta}}^i$ are the displacement, velocity, angular displacement and angular velocity, respectively. The subscripts 'j' refers to the jth neighboring block. n is the block number which is neighboring of ith block, and n' the Lp points on the ith block. $P^{i,l}$ is fissure water pressure at the ith Lp point on the ith block, $\vec{F}$ the external force such as gravity, and $\vec{M}$ the external moment. r_0 is the rotating radius and $\vec{r}_l$ the vector from mass center to Lp point.

(2) Force-displacement relation (physical equation). The force-displacement relation at the LP point is used to express the interaction of two blocks. When two blocks contact each other, this relation can be expressed in normal and tangential directions, respectively, as follows:

$$\Delta F_n = -k_n A_s \Delta u_n, \tag{5}$$

$$\Delta F_s = -k_s A_s \Delta u_s, \tag{6}$$

where ΔF_n and ΔF_s are the increments of normal and tangential forces at the LP point, and Δu_n and Δu_s the corresponding displacement increments. k_n and k_s are the normal and tangential stiffness respectively, and A_s the area of the Lp zone.

When the interface is open ($F_n+P>\sigma_t^i A_s$), the forces on the interface are all zeros:

$$F_n = 0, \tag{7}$$

$$F_s = 0. \tag{8}$$

When the interface is sliding $(F_s > CA_s + F_n \tan\phi)$, the forces on interface observe Mohr-Coulomb's law:

$$F_s = F_n \tan\phi, \tag{9}$$

where F_n and F_s are normal and tangential forces at the LP point. C is the cohesion on the interface, ϕ the frictional angle, σ_t^j tensile strength on the interface, and P the fissure water force at the LP point.

3.3 Computation parameters and boundary conditions

Maximum dimension is x_l=2.0 m, y_l=0.3 m and z_l=1.2 m in numerical simulation. The friction angle varies from 18 to 21 degree. Table 2 summarizes the mechanical properties of rock blocks and joints and Table 3 is the geometrical parameters of joints in which β is the slope angle. The layers except fixed bottom layer do not contact with sidewalls. Such a slope has following boundary conditions: zero displacement is given to the blocks on bottom layer. Fig. 3 is the distribution of block centers in computation.

Table 2 Mechanical properties of rock blocks and joints

Properties of blocks			Strength and stiffness of interface			
Density /kg·m^{-3})	Poisson ratio	E/N·m^{-2}	C/Pa)	ϕ/°	k_n/N·m^{-3}	k_s/N·m^{-3}
2700	0.2	6.75×10^{10}	0	19.5	3.375×10^{11}	3.375×10^{11}

Table 3 Geometrical parameters of joints

Joint set	Granite(20 mm×10 mm×10 mm)		
	Space/m	Angle/°	Orient./°
1	0.2	90–β	0
2	0.1	90	90
3	0.1	β	180

3.4 Comparison of numerical simulations with experimental observations

DEM simulations are compared with two experimental observations in Figs. 4 and 5. Failure modes simulated by DEM are in good agreement with experimental observations.

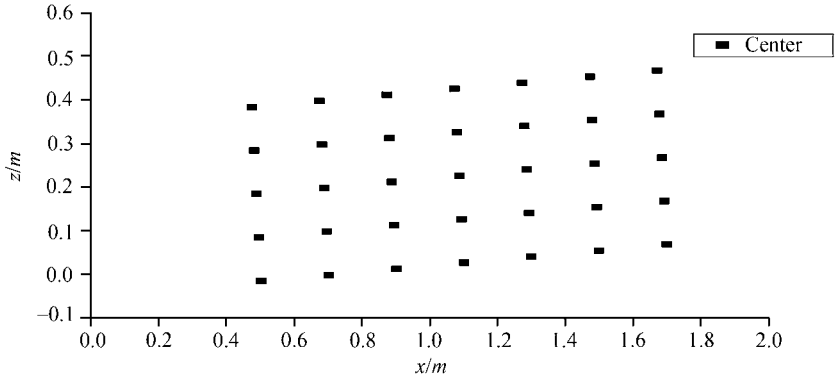

Fig. 3. Block center distribution.

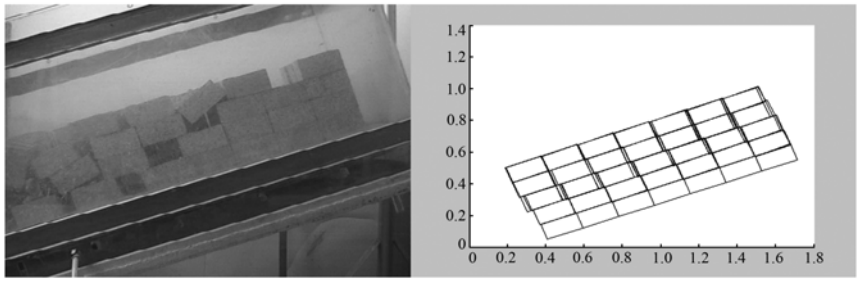

Fig. 4. Comparison of numerical simulation results with experimental photo in the state of no watering.

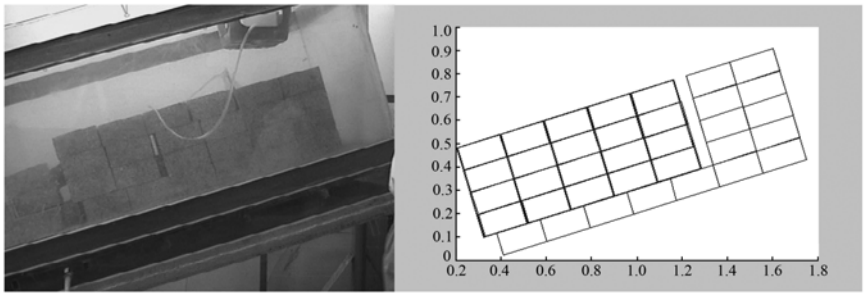

Fig. 5. Comparison of numerical simulation results with experimental photo in the state of watering in the fifth fracture.

We define L as the distance between water-holding fracture in vertical sliding surface and slope toe and H as the depth of fissure water. It is interesting to plot the L/H versus the critical angle in Fig. 6, where circular dots are experimental results, triangle dots are DEM simulations, and straight line denotes the critical angle when fracture is dry.

As seen from Fig. 6, when the first fracture is watered, the fissure water pressure strongly affects the critical angle of slope. The greater the distance becomes, the closer the experimental critical angle is to the critical angle when fracture is dry. When the ratio is over three, the effect of fissure water pressure on the critical angle of landslide is ignorable. When L increases, the push force from fissure water remains the same but

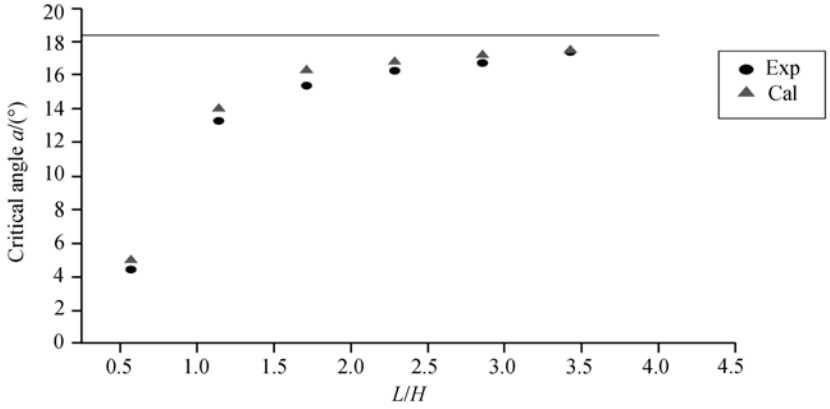

Fig. 6. Comparison of numerical simulation results with experimental measurements.

frictional force increases due to longer sliding surface. This makes the fissure water pressure affect the critical angle less and less and failure modes of slope change correspondingly. Again, numerical simulations are in agreement with experimental measurements. This implies that current three-dimensional discrete element face-to-face contact model with fissure water pressure is suitable and reliable. It can accurately compute the critical angle of jointed slope when the effect of fissure water pressure in vertical sliding surface is taken in account.

4 Theoretical analysis for fissure water pressure

4.1 Factor of safety

This section will quantitatively analyze the effect of vertical fissure water pressure on landslide stability through a slope in Fig. 7. The location of structural surface is an important parameter. Take a sliding block for consideration. The force from its back blocks is marked as P_x when fracture is dry. The normal force on sliding surface is denoted as $P_{y.}$ Then friction force f on the sliding surface is

$$f = \tan\phi \int_0^x P_y(y)dx, \tag{10}$$

$\tan\ \phi$ —friction coefficient.

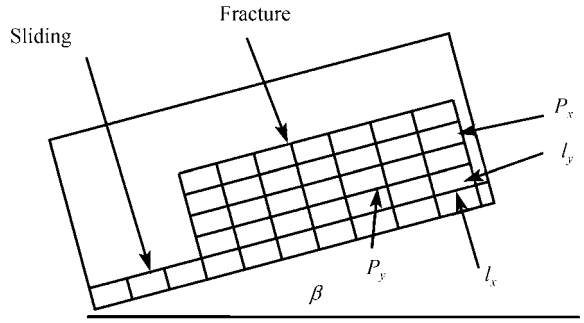

Fig. 7. Talus sketch map.

Body forces P_{vx} and P_{vy} of this sliding body are as follows:

$$P_{vx} = \iint_v \rho g_x dxdy = \iint_v \rho g \cdot \sin a \cdot dxdy = \rho xyg \cdot \sin \beta, \tag{11}$$

$$P_{vy} = \iint_v \rho g_y dxdy = \iint_v \rho g \cdot \cos a \cdot dxdy = \rho xyg \cdot \cos \beta, \tag{12}$$

x, y —location of structural surface.

Safety coefficient K is the ratio of anti-slide force to up-down sliding force

$$K = \frac{C^{ij}x^i + \tan\phi \int_0^x P_y(y)dy}{P_{vx} + \int_{h-y}^h P_x dy}. \tag{13}$$

Take $y = h - y'$. y' denotes the depth of fractured water in vertical sliding surface

$$K = \frac{C^{ij}x^i + \tan\phi \int_0^x P_y(y')dx}{P_{vx} + \int_0^{y'} P_x dy'} = \frac{C^{ij}x^i + \tan\phi \int_0^x P_y(y)dx}{P_{vx} + \int_0^y P_x dy}, \tag{14}$$

x', y'—location of structural surface studied,

C^{ij} — bonding strength in *i*-*j* surface.

From eq. (14) we can see two points: 1) If the cohesion strength is not considered (C is equal to 0), safety coefficient is independent of gravity; 2) safety coefficient is the coefficient of stability in structural surface x' and y'. It is obtained to minimize the coefficient of stability in all structural surfaces. That is, the minimum K among all structural surfaces is the safety coefficient in whole slope. If the C is not zero such as non-connected surface, the safety coefficient is big and the surface may not be dangerous surface. We can calculate the safety coefficients for all structural surfaces and the structural surface with minimum safety coefficient is the sliding surface.

4.2 Push action of water pressure

The safety coefficient K for dry fracture (C is equal to 0) is

$$K = \frac{\tan\phi \int_0^x P_y(y)dx}{\rho gxy \sin\beta} = \frac{\tan\phi}{\tan\beta}. \tag{15}$$

After filling water into fracture, the stability coefficient is

$$K = \frac{\tan\phi \int_0^x P_y(y)dx}{\rho g\left(xy\sin\beta + \dfrac{\rho_w \cos\beta}{\rho}\int_0^y P_x(y)dy\right)} = \frac{\tan\phi}{\dfrac{\rho_w}{2\rho}g\dfrac{y}{x} + \tan\beta} \tag{16}$$

Comparing formulas (15) and (16), it is found that anti-slide force is invariable whether fissure water exists or not. When the fracture in vertical sliding surface is full of water, the rock slope is in its limit equilibrium. That is,

$$\tan\phi - \tan\beta = \frac{\rho_w}{2\rho} g \frac{y}{x}. \tag{17}$$

If $\rho = 2.7\rho_w$ and $3y \leqslant x$, $\tan\phi - \tan\beta \leqslant 0.06$. It is noted that the $\tan\phi = \tan\beta$ for dry fracture which can be obtained from eq. (15). The above result means that if the relative position of fissure water *y/x* is three times larger, the pushing force from fissure water pressure can be ignorable within the error of 6%. In other words, the fissure water in vertical sliding surface has little effect on the critical angel of landslide. This is in agreement with the experiment results.

5 Effect of multi-water-holding fractures far away from slope toe on slope stability

Numerical simulation is carried out by the DEM to study the effect of multi-water-holding fractures. The study area is increased to twelve rows of blocks. The distribution of block centers in numerical simulation is shown in Fig. 8, and the parameters in Tables 2 and 3 are used. Only the bottom blocks are fixed. Friction angle is taken as the mean of 18—21 degrees. Critical angle is calculated in two cases, one is that only the seventh fracture is filled with water, the other is that water fills the seventh, eighth, ninth, tenth fractures simultaneously.

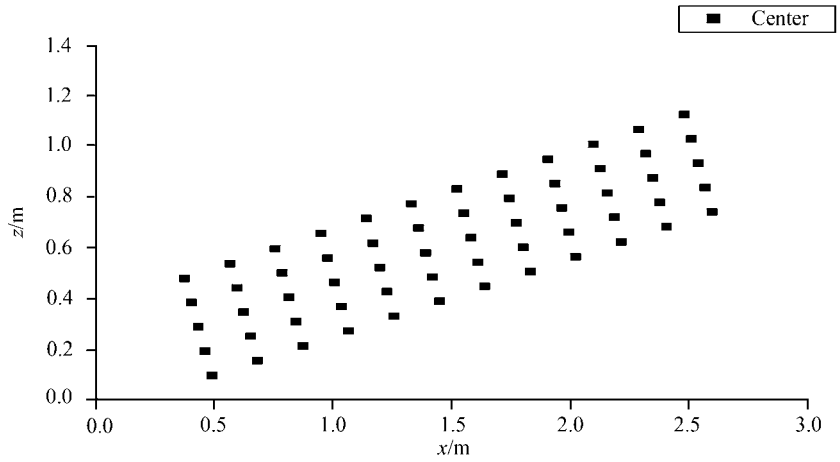

Fig. 8. Block center distribution.

The critical angle is 17.8 degree for the case that only the seventh fracture is filled with water, and is 17 degree for other case. This result again shows that water filling those fractures beyond the distance between fracture and slope toe three times more than

the depth of fracture has little effect on critical angle. Fracture is dense at the back of slope and the distance between fracture and the slope toe is three times greater than the depth of fracture. When $\Delta H/\Delta L \leqslant 3$ (ΔH is the water head difference and ΔL is the distance between two adjacent filling fractures), the slope at that location will reach its limit equilibrium first. If the local sliding occurs, the front slope will be pushed and affects the critical angle. However, when two fractures in our experiment are filled with water but their water heads are the same, the critical angle is not affected.

6 Conclusions

(1) The results of experiment investigation, numerical simulation and theoretical analysis all show that the ratio of the distance between water-holding fracture and slope toe to the depth of fissure water is a key factor to the critical angle of landslide. Our experimental results show that the ratio is three times greater, the effect of fissure water pressure in vertical sliding surface on the critical angle of landslide can be ignored.

(2) Current DEM simulations are in good agreement with experimental observations for failure mode and process. This proves that the current three-dimensional discrete element face-to-face contact model with fissure water pressure is suitable and reliable. It can accurately predict the critical angle regardless of existence of fissure water in vertical sliding surface.

(3) Experimental observations show that failure modes have sliding, toppling, or their combination. We cannot simply use single criterion of sliding and toppling as limiting equilibrium. The discrete element method can complexly describe slipping, rotating and toppling in the course of slide destabilization.

Acknowledgments This work was supported by the National 973 Project (Grant No. 2002CB412703), and the Important Aspect Project of the Chinese Academy of Sciences (Grant No. KJCX2_SW_L1).

References

1. Yan Lin, Li Shihai, Dong Dapeng et al., The discrete element numerical simulation for Wulong landslide, Mechanics and Practice, 2002, 24 (suppl.): 94－99.
2. Braathen, A., Blikra, L. H., Berg, S. S. et al., Rock-slope failure in Norway; type, geometry, deformation mechanisms and stability, Norwegian J. of Geology, 2004, 84(1): 67－88.
3. Garinger, B., Alfaro, M., Graham, J. et al., Instability of dykes at Seven Sisters Generating Station, Canadian Geotechnical Journal, 2004, 41: 959－971.
4. Cappa, F., Guglielmi, Y., Soukatchoff, V. M. et al., Hydromechanical modeling of a large moving rock slope inferred from slope leveling coupled to spring long-term hydrochemical monitoring: example of the La Clapiere landslide (Southern Alps, France), J. of Hydrology, 2004, 291: 67－90.
5. Mikos, M., Cetina, M., Brilly, M., Hydrologic conditions responsible for triggering the Stoze landslide, Slovenia, Engineering Geology, 2004, 73: 193－213.
6. Wang, J. G., Investigation on the method of middle and short prognosis of landslides, J. of Chongqing University, 1991, 14(3): 67－72.
7. Sun Guangzhong, Rock Structural Mechanics, Beijing: Science Press, 1988.
8. Wu Yanqing, Zhang Zhuoyuan, Introduction to Rock Hydraulics, Chengdu: Southwest Jiao Tong University Press, 1995.

9. Chai Junrui, Wu Yanqing, Double mechanical effect of fracture flow on fracture wall in rock, Rock and Soil Mechanics, 2003, 24(4): 514－517.
10. Wu Yanqing, Chai Junrui, Analysis of seepage force on rock fracture network, Engineering Geology, 2001, 9(1): 24－28.
11. Jidian Zhang, Shiwei Bai, Effect of seepage pressure on jointed fracture rock slope[J], Western Exploration, 2003, (2): 4－6
12. Shen Zhujiang, Not taking fiction as truth－phenomenon anatomy of concept confusion in the field of rock and soil engineering, Journal of Chinese Geotechnical Engineering, 2003, (6): 767－768.
13. Sun Yong, The effect and quantitative evaluation of fractured water in the stability of rock slope, War Industry Reconnaissance, 1993, (4): 28－32.
14. Li, S. H., Lian, Z. H., Wang, J. G., Effect of rock mass structure and block size on the slope stability—— Physical modeling and discrete element simulation, Science in China, Ser. E, 2005, 48(supp.): 1－17.
15. Li Shihai, Wang Yuannian, Three-dimensional discrete element soil-rock stochastic model and numerical simulation of unidirection loading experiment, J. of Chinese Geotechnical Engineering, 2004, 26(2): 172－177.